ACS Chemical Neuroscience pubs.acs.org/acschemicalneuroscience Article

Quantum Dot Labeling of Butyrylcholinesterase Maintains Substrate and Inhibitor Interactions and Cell Adherence Features

Nir Waiskopf,[†,‡] Itzhak Shweky,[†] Itai Lieberman,[†] Uri Banin,*[,†] and Hermona Soreq*[,‡]

[†]The Institute of Chemistry and the Center for Nanoscience and Nanotechnology and [‡]The Alexander Silberman Institute of Life Sciences and the Edmond and Lily Safra Center for Brain Sciences, The Hebrew University of Jerusalem, Edmond J. Safra Campus, Givat Ram, Jerusalem 91904

Abstract

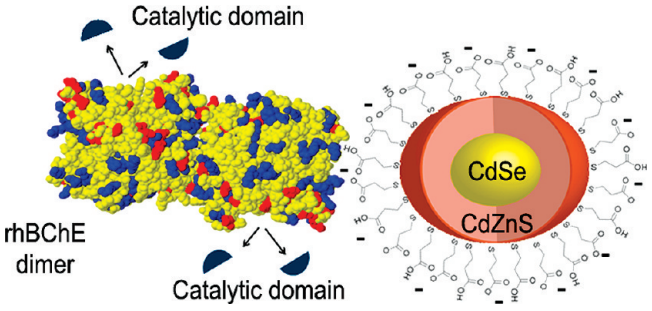

Butyrylcholinesterase (BChE) is the major acetylcholine hydrolyzing enzyme in peripheral mammalian systems. It can either reside in the circulation or adhere to cells and tissues and protect them from anticholinesterases, including insecticides and poisonous nerve gases. In humans, impaired cholinesterase functioning is causally involved in many pathologies, including Alzheimer's and Parkinson's diseases, trait anxiety, and post stroke conditions. Recombinant cholinesterases have been developed for therapeutic use; therefore, it is important to follow their in vivo path, location, and interactions. Traditional labeling methods, such as fluorescent dyes and proteins, generally suffer from sensitivity to environmental conditions, from proximity to different molecules or special enzymes which can alter them, and from relatively fast photobleaching. In contrast, emerging development in synthesis and surface engineering of semiconductor nanocrystals enable their use to detect and follow molecules in biological milieus at high sensitivity and in real time. Therefore, we developed a platform for conjugating highly purified recombinant human BChE dimers (rhBChE) to CdSe/CdZnS quantum dots (QDs). We report the development and characterization of highly fluorescent aqueous soluble QD-rhBChE conjugates, present maintenance of hydrolytic activity, inhibitor sensitivity, and adherence to the membrane of cultured live cells of these conjugates, and outline their advantageous features for diverse biological applications.

Keywords: Anticholinesterases, bioconjugation, butyrylcholinesterase, confocal microscopy, quantum dots, transmission electron microscopy

Butyrylcholinesterase (BChE) is a serine hydrolase which degrades the neurotransmitter acetylcholine (ACh) and is thus involved in the regulation of cholinergic signaling (*1*−*4*). BChE functions in both the brain and peripheral systems of all vertebrates, where it adheres to cholinergic synapses and neuromuscular junctions (*5*−*10*). BChE is a key natural protector from poisonous anticholinesterase agents, and carriers of debilitated BChE mutants show hypersensitivity to both anticholinesterase therapeutics (*11*) and agricultural insecticides (*12*, *13*). BChE further appears to contribute to lipoprotein metabolism (*14*) and cellular adhesion (*15*). Correspondingly, impaired BChE functioning is presumably involved in many pathologies, including Alzheimer's (*16*−*18*) and Parkinson's diseases (*19*, *20*) and trait anxiety (*21*, *22*). Therefore, numerous studies are done to reveal BChE's in vivo path, location, and interactions, and recombinant BChEs have been developed for research and therapeutic use (*18*). To detect and track BChE molecules in biological milieus at high sensitivity and in real time, an appropriate platform is needed. The use of fluorescent dye labeling to track BChE for therapeutic and biological applications highlighted BChE interactions as being an imminent element in the in vivo roles of this enzyme (*23*); however, limited photostability and relatively small nonlinear absorption cross sections prevented its use for fluorescence labeling in imaging modalities such as two-photon microscopy (*24*−*26*). Moreover, the traditional labeling methods with fluorescent proteins and dyes generally suffer from sensitivity to environmental conditions and from proximity to different molecules and enzymes. Temperature, pH,

Received Date: August 31, 2010
Accepted Date: November 27, 2010
Published on Web Date: December 14, 2010

DOI: 10.1021/cn1000827 | *ACS Chem. Neurosci.* (2011), *2*, 141–150

solvent polarity, presence of chloride, or proteases that can degrade the fluorescent proteins and dyes are only a few examples of parameters which can affect their efficiency (*26*−*29*). Therefore, we initiated a search for a more efficient labeling platform which would sustain the enzymatic and biological qualities required for BChE research and application purposes.

A new and powerful approach for state-of-the-art biological and medical research emerges from synthesis and surface engineering of diverse nanoparticles. Colloidal semiconductor nanoparticles, quantum dots (QDs), enable unprecedented advantages for high sensitivity multilabeling in vitro and in vivo (*26*, *30*, *31*). In comparison to other fluorescent agents, QDs have the same order of magnitude or even higher quantum yield (QY) (*26*, *32*), higher molar extinction coefficients (*33*, *34*), broader absorbance that increases toward shorter wavelengths, and controlled size-dependent narrow photoluminescence spectra which allow broad selection of the excitation wavelength and thus separation of excitation and emission. Moreover, QDs are better amenable than other fluorescent agents, for dynamic high resolution imaging of intra- and extracellular interactions in real time, and open new opportunities for direct follow-up of numerous biological processes (*30*, *31*) due to their higher thermal and photochemical stability which enable extended detection time (*35*−*37*). The QDs can be surface coated by polymers (*38*, *39*), silica (*40*), or organic ligands (*24*). The surface coating plays a crucial role in the biocompatibility of the QDs. It determines the stability of the QDs in different pH conditions and salt concentrations by electrostatic repulsion, steric exclusion, or a hydration layer on the surface which prevent aggregation (*41*−*43*), affect their fluorescence QY due to electronic passivation, and may reduce their cytotoxicity (*42*). Moreover, the surface coating can determine the conjugation between the QDs and the biological molecules because the conjugation process depends on the chemical and physical properties of both of them. Different chemical groups on protein surfaces as well as on the surface coating of the QDs enable use of diverse bioconjugation techniques which can be classified by their nature and strength. The major techniques are direct conjugation, affinity based ligand−receptor conjugation, and electrostatic and covalent conjugation. Direct techniques include conjugation of the biomolecule directly to the QDs' metals as a ligand, for example, conjugation of nucleic acids modified with thiol groups (*44*) or peptides modified with cysteines (*45*) that have high affinity to the QDs. This conjugation procedure is used mostly for small biomolecules which are easily modified. For bigger molecules, affinity based ligand−receptor conjugation, using QDs−antibody for specific site binding (*24*) or use of QDs−avidin for the recognition of biotinylated biomolecule (*46*), is the most specific technique. However, these mediate molecules which provide specificity to the bioconjugates are also responsible for their disadvantages: enlargement of the distance between the QDs and the biomolecule and magnification of the bioconjugates size. These may interfere with experiments involving intracellular delivery or fluorescence resonance energy transfer. An easy alternative if possible is electrostatic conjugation, which can be used when the biomolecule has a strong global charge that can direct its binding to an oppositely charged surface-coated QD (*47*). However, there may be limitations to this straightforward conjugation approach. Sometimes, the binding interaction is not strong enough under physiological conditions. In these cases, covalent conjugation can be used, where a covalent bond is created between special chemical groups on the QD surface and on the biomolecules with or without homobifunctional or heterobifunctional cross-linker (*48*).

Even given this wide range of conjugation techniques, the dependence on the protein solubility and function as well as on the colloidal stability of the QDs in different environmental conditions limits the feasible conjugation routes. These constrains are enhanced when dealing with labeling of enzymes, where maintenance of catalytic activity and susceptibility for inhibition is sought or when toxicity should be taken into account. For these reasons, the preparation of QD-labeled enzymes must be specifically designed for each enzyme independently and should span both catalytic activity and toxicity tests.

Here we report the development and characterization of QD-rhBChE conjugates. Conjugation of highly purified recombinant human BChE (rhBChE) dimers to QDs was selected since the resultant QD- rhBChE conjugates are amenable for in vitro and in vivo imaging as well as for use as biosensors.

Results and Discussion

CdSe/CdZnS core/shell semiconductor nanocrystal QDs were prepared by modification of a previously described synthesis protocol (*49*) and were initially capped with trioctylphosphine oxide (TOPO) and oleic acid (Supporting Information). An emission spectrum with a peak at 626 nm (Figure 1A) was detected for these QDs, with a high fluorescence QY of 60−70% in toluene. Their size, as measured in transmission electron microscopy (TEM) images, revealed a narrow size dispersion and overall diameter of 10 ± 1 nm (N = 300 particles, Figure 1B). To render the NPs useful for biological labeling, we used ligand exchange to transform the coating of the NPs from hydrophobic to hydrophilic. We selected mercaptopropionic acid (MPA) as the working ligand and performed ligand exchange following modification of a previously described protocol (*44*, *50*). The fluorescence QY in water was only

DOI: 10.1021/cn1000827 | *ACS Chem. Neurosci.* (2011), *2*, 141–150

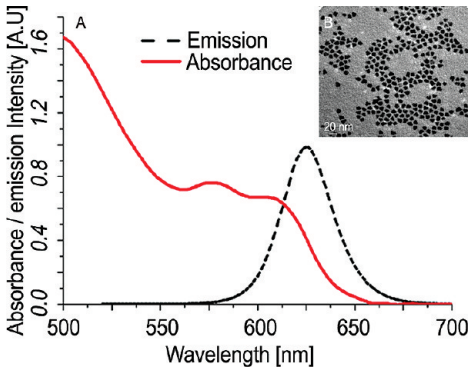

Figure 1. Characterization of the CdSe/CdZnS QDs. (A) Absorbance (red) and emission spectra (black, dashed line) of the QDs in toluene. The excitation and emission peaks were at 610 and 626 nm, respectively. (B) TEM image of the QDs with average size of 10 ± 1 nm in diameter.

slightly reduced from that within the organic solvent, typically by 10%.

Conjugation and Characterization of the QD-rhBChE Conjugates

About 25% of the native BChE weight is contributed by nine asparagine-linked carbohydrate chains per subunit (*51*). The terminal carbohydrate is the negatively charged sialic acid, with 72 sialic acids per tetramer yielding an isoelectric point of approximately 4 for native BChE. However, in our study, we conjugated by adsorption to the QDs in water, highly purified recombinant human BChE dimers (rhBChE) produced in the milk of engineered goats. This protein carries far less sialic acid residues than the native protein, and its negative charge is hence considerably lower (*52*). The adsorption was enhanced when the working pH was reduced. However, at pH < 5.5, the QDs tend to aggregate due to the protonation of the thiolate ligands, which limits the repulsive force between them. Based on these considerations, a straightforward conjugation procedure was developed in which rhBChE dimers were adsorbed to the QDs in triple distilled water (TDW, pH = 6). Following this, the conjugated system was characterized by various methods. First proof for the effective conjugation of the QDs to rhBChE was obtained by electrophoresis of the conjugation products under nondenaturing conditions in agarose gels. Additionally, this gel electrophoresis procedure provided means to separate between conjugated and nonconjugated components and characterize the properties of these QD-rhBChE conjugates. Two distinct fluorescing QD bands were readily observed under exposure of the gel to UV light (312 nm), whereas loading these gels with unconjugated QDs alone showed a single major band. This provides evidence that a major fraction of the QDs was effectively conjugated to the rhBChE dimers. Supporting this observation, QD-rhBChE prepared using a 1:10 QDs-rhBChE ratio yielded a narrow and sharp

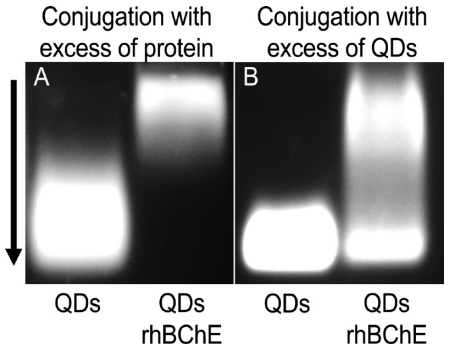

Figure 2. UV fluorescence of slowly migrating electrophoretically separated QD-rhBChE conjugates. (A) QD-rhBChE conjugates prepared under conditions of rhBChE excess. Note slow migration compared to unconjugated QD controls. (B) QD-rhBChE conjugates prepared under QDs excess. Note smeared fluorescent band including both conjugates and free QDs.

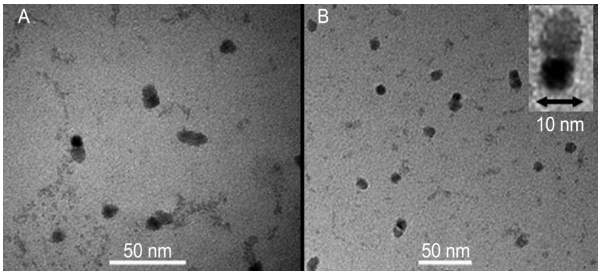

Figure 3. TEM images of QD-rhBChE conjugates. (A) Positive staining with uranyl acetate of QD-rhBChE 1:1 conjugates. (B) QD-rhBChE conjugates in a different field on the grid. The inset is a magnification of one of the conjugates; the dark area is the QD, while the lighter area is rhBChE.

band with a slower migration profile than that of the QDs band (Figure 2A), apparently due to the smaller charge to size ratio. Also, a QDs-rhBChE excess ratio (over 2:1) yielded a smeared band which migrated at a range spanning both the conjugates and the QD bands (Figure 2B), providing a coarse estimation of the ratio between conjugated and nonconjugated QDs in the sample.

During this analysis, we found that the hydrolytic activity of rhBChE is sensitive to the UV exposure (312 nm, 0.02 W/cm^2) used for these detections (Supporting Information). To selectively detect possible reductions caused by the conjugation itself, we ran a reference sample in a parallel lane on the gel and avoided exposing this lane to the UV light. UV-exposed samples served for detection purposes, whereas unexposed samples from the reference lane were employed for the following steps.

Direct visualization of the QD-rhBChE conjugates involved TEM analysis following positive staining with uranyl acetate (Figure 3). Uranyl acetate staining yields high contrast in the protein part of the conjugates. The images show the presence of two segments with different contrast, a dark one corresponding to the QD and a lighter one corresponding to the stained rhBChE. This directly demonstrated the presence of 1:1 QD-rhBChE

DOI: 10.1021/cn1000827 | *ACS Chem. Neurosci.* (2011), *2*, 141–150

conjugates. No such conjugates were seen in control samples of QDs or rhBChE alone. Antibodies, alone or conjugated to metal NPs, are often used to obtain additional, independent identification of electrophoresis and TEM studied proteins. However, in the current electrophoresis experiments, we used a pure recombinant protein and employed catalytic activity measurements with all of the relevant controls to confirm that the extracted protein was rhBChE. Also, in the TEM study, we were concerned that antibody labeling would have hampered the ability to extract information from the TEM pictures due to the limited resolution offered by this method. Thus, the diameter of the bound protein was estimated from the image to be close to 10 nm, smaller than the diameter of antibodies and compatible with the crystallography findings (*53*).

The conjugation process involved specific pH and salt concentrations which are different from those of the physiological environment. However, the conjugates presented satisfactory stability and lack of aggregation under physiological conditions (0.1 M pH 7.4 phosphate buffer) for up to 72 h after the gel electrophoresis procedure, highlighting their suitability for extended in vitro and in vivo experiments. Additionally, although our work has been focused on CdSe-based QDs, the observed conjugation was also seen with InP-based QDs. This demonstrates the applicability of this conjugation approach to serve as a wider platform for diverse kinds of semiconductor QDs.

Catalytic Activity and Inhibition Tests

One of the issues in the use of unspecific site conjugation is the possibility that the conjugation will modify the electric field surrounding the conjugated protein, interfere with substrate and inhibitor accessibility to the active site of the enzyme, and prevent its hydrolytic activity features. To address this issue, the conjugates were first cleaned from free proteins and ligands. Bands were cut from the agarose gel and transferred to dialysis bags, and the samples were extracted by subjecting these bags to an electric field. The catalytic activity of each extract was measured by the spectro-photometric Ellman's assay (*54*) using butyrylthiocholine as substrate of rhBChE and dithionitrobenzoate (DTNB) as a degradable prodye. The extracted conjugates, but not control extraction samples from a parallel migrating empty band, nor the QDs migrating band, showed reproducible catalytic activity (Figure 4A). This implied that the stable conjugation products maintained enzymatic activity. To avoid interaction of the free ligands with the degradable dye, we compared the catalytic activity in fully loaded conjugates (10:1 QD-rhBChE ratio) purified by dialysis to that of free protein samples. Ellman's assay measurements showed 50% catalytic activity of that of comparable amounts of similarly treated free rhBChE (Figure 4B). The reduced activity could potentially reflect fully maintained activity

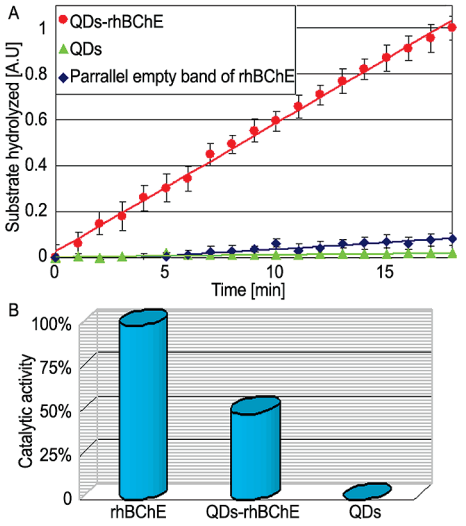

Figure 4. QD-rhBChE conjugates maintain catalytic activity. (A) Extract from the conjugate band but not the extract from a similarly migrating empty band of rhBChE sample or the QDs band showed catalytic activity. *Y* axis: Arbitrary units of spectrophotometric absorbance. (B) Catalytic activity of conjugates prepared with excess of QDs over rhBChE was 50% of that of free rhBChE subjected to the same process. Control samples with QDs alone did not show any catalytic activity.

of one out of the two monomers in each dimer, suggesting that the conjugation involved only one of the subunits. Alternatively, both subunits may have lost part of their hydrolytic activity due to the relatively large size of the QDs and the direct interaction between the QDs and rhBChE. Of note, the reduction in catalytic activity of the rhBChE protein may limit its use. Minimization of the conjugation effect on rhBChE functions might possibly be achieved using smaller QDs or by covalent conjugation through molecular linkers that will enlarge the distance between the QDs and the rhBChE molecules. However, further experimental validation will be required to find out if one or more of these steps will sustain higher catalytic activity of the QD-rhBChE conjugates.

Conjugate Structure and Catalytic Activity Considerations

After establishing the formation of conjugates and their enzymatic activity, we next demonstrate further expansion of the method to other QDs systems and QD ligands. Conjugation experiments with different QDs systems such as CdSe/CdS, CdSe/ZnS, and InP/ZnS core/shell nanocrystals showed similar adsorption to the rhBChE which implies primary dependence on the QDs surface coating. This allows labeling of rhBChE with other QD systems that can have emission peaks in desirable wavelengths, and in particular in the near-infrared which is important for in vivo experiments due to tissue absorbance in the visible range. This can also allow the use of QDs without cadmium that can be toxic to the biological systems and enables labeling with

DOI: 10.1021/cn1000827 | *ACS Chem. Neurosci.* (2011), *2*, 141–150

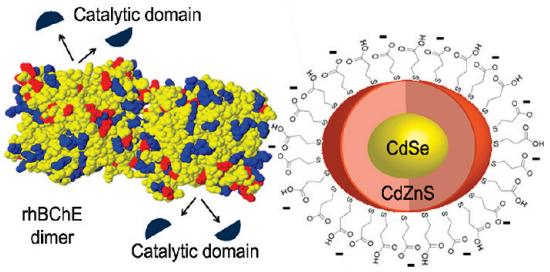

Figure 5. Scheme of the QD-rhBChE conjugates. Adsorption of rhBChE dimers to CdSe/CdZnS core/shell QDs with MPA as a ligand. The carboxyl groups on the QDs attract the basic residues (blue) on rhBChE's surface. Arrows mark the active site gorge where ACh gets hydrolyzed.

semiconductor nanoparticles of different sizes and shapes, potentially limiting the reduction in catalytic activity of these QD-rhBChE conjugates. Adsorption being affected by pH implies that electrostatic forces play important role in the conjugation. Of note, insight on the adsorption site which is crucial for maintaining the enzymatic activity and inhibitor susceptibility may be obtained from evaluation of the charge distribution on the rhBChE surface taken from its protein database (PDB: 2pm8) (*53*). Marking the basic and acidic residues on rhBChE surface in blue and red, respectively, identified a positively charged domain far from either the dimerization or the catalytic sites (Figure 5). We may infer that the negatively charged QDs will adhere preferentially to this positive site on rhBChE surface. This model does not take into account the nine BChEs' glycosylation sites which contribute negative charged carbohydrate chains. However, rhBChE in comparison to serum BChE is underglycosylated and its carbohydrate chains are less charged (*52*); therefore, the glycosylation effect is minimized.

Our experiments with different mercaptocarboxylic ligands imply that the presence of negative carboxylic groups on the QDs surface provide effective binding to the protein. This was well demonstrated by conjugation of QDs with glutathione as a ligand to rhBChE using a similar procedure as with the MPA ligand. Glutathione-coated QDs maintain a higher fluorescence QY, have colloidal stability in wider pH range and salt concentration in comparison to MPA coated QDs, and are more biocompatible (*42*, *43*, *55*−*57*).

After the conjugation, the QD-rhBChE conjugates were subjected to hydrolytic activity and inhibitor susceptibility tests. Fractions were separated by gel electrophoresis and extracted from the gel by dialysis. Activity was determined following 20 min preincubation with or without 0.5 mM paraoxon, the metabolite of the pre-insecticide parathion. Ellman's assay measurements showed reduction of 90% and 80% in the catalytic activity of treated free enzyme or QD-rhBChE conjugates, in comparison to matched untreated preparations

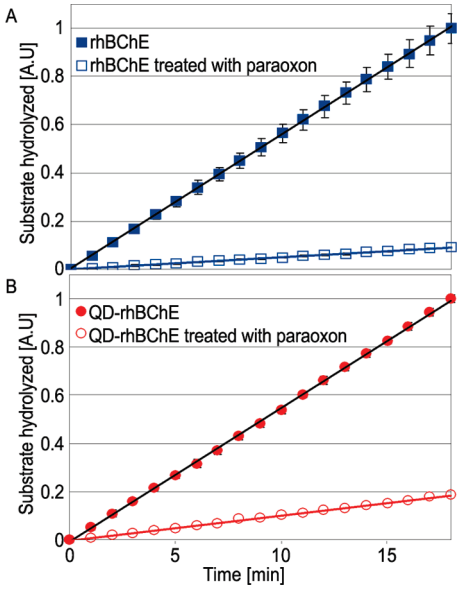

Figure 6. Paraoxon inhibits QD-rhBChE catalytic activity. (A) Ellman's assay measurements showed a decrease of 90% in the catalytic activity of free enzyme after treatment with paraoxon (empty squares) in comparison to untreated preparation (full squares). (B) Ellman's assay measurements showed a decrease of 80% in the catalytic activity of QD-rhBChE after treatment with paraoxon in comparison to untreated QD-rhBChE (full circles). Data shown is mean ± S.E. of triplicates.

(Figure 6). These results strengthen the conjecture that the active site gorge, to which both the substrate and the inhibitors are attracted (*58*), is occluded in part by the QD-bound enzyme.

Labeling BChE−Cell Membrane Interactions

Apart from its hydrolytic activity, BChE is known to adhere to cell membranes (*59*, *60*), where it terminates cholinergic signaling (*18*, *61*). It also hydrolyzes ACh in the circulation, where it is the major cholinesterase (*11*). However, viewing BChE−cell interactions traditionally requires fixation, and to the best of our knowledge this has not been performed previously in live cell preparations. BChE is associated with endothelial cells as well as with glial cells and neurons (*4*, *62*, *63*), and debilitated BChE variants confer added risk of acute ischemic stroke (*64*); therefore, to test if the QD-rhBChE conjugates maintained this membrane interaction capacity and view it in live cells, we incubated QD-rhBChE conjugates with cultured bEnd.3 mouse brain microvascular endothelial cells (ATCC number: CRL-2299). The inherent fluorescence properties of these QD-rhBChE conjugates served to examine possible interaction with the live cell membrane. Briefly, cell samples were incubated in multiwell plates for 3 h with 10 μL of 100 nM purified QD-rhBChE, followed by incubation with Hoechst 33342 (nuclear DNA marker-blue). Confocal microscopy was then used to localize the QD-rhBChE on the *Z*-axis of the labeled cells (Figure 7). Serial

DOI: 10.1021/cn1000827 | *ACS Chem. Neurosci.* (2011), *2*, 141–150

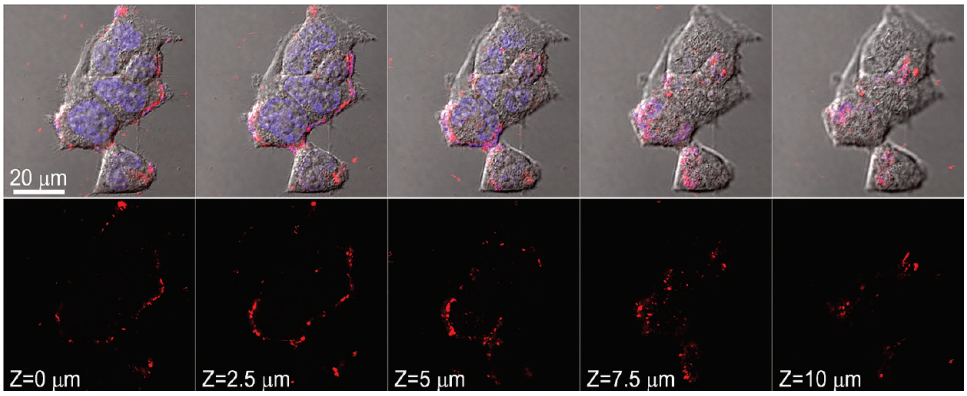

Figure 7. QD-rhBChE conjugates adhere to the membranes of live cells. Shown are confocal microscopy cross section photographs of bEnd.3 microvasculature endothelial cells incubated with QD-rhBChE (red) and with the nucleus marker Hoechst 33342 (blue). Merging of transmission and luminescence images (upper row) and luminescence images of the QD-rhBChE conjugate (lower row) demonstrate rings of QD-rhBChE surrounding those cell membranes which remained exposed to the culture environment and converged as going up in the *Z*-axis. These results demonstrate that the QD-rhBChE conjugates interact with accessible cell membrane sites.

sections of these confocal images showed converging rings of QD-rhBChE (red) with increasing *Z* values, corresponding to the contour of the cell membranes. Importantly, only those membranes exposed to the environment were labeled, whereas those separating between adhered cells remained unlabeled (Figure 7). This observation demonstrated that the QD-rhBChE conjugates maintained their capacity to interact with the cell membrane but did not penetrate the membrane. Moreover, MTT cell viability assay demonstrated that the volume and concentration of the QDs that were used in our experiments did not cause cell death, consistent with previous cytotoxicity tests of similarly composed QDs with MPA as surface coating (*65*).

Conclusion

In this study, we introduce a general method for QD labeling of rhBChE based on adsorption. This labeling yields a stably labeled, catalytically active and inhibitor sensitive rhBChE with the advantage that QD labeling can offer longer photostability, lower sensitivity to the chemical environment, better suitability for different optical measurements, and the possibility to follow the dynamics of this protein's interaction with the cell membrane in live cells, to name a few. These advantages make these conjugates suitable for use in studies addressing key biological questions in ways that were not available before, may hopefully yield better understanding of the underlying mechanisms of diseases with which BChE is associated, and open new venues to improved applications for diagnosis, treatment, and prevention modalities for such diseases.

Methods

Reagents

Mercaptopropionic acid (MPA), potassium hydroxide, anhydrous toluene, Trizma base, *S*-butyrylthiocholine iodide (BThCh), 5,5′-dithio-bis(2-nitrobenzoic acid) (DTNB), acetic acid, methanol, uranyl acetate, paraoxon, dialysis tubing cellulose membrane, and L-glutamine were obtained from Sigma. Highly purified recombinant human BChE was from Pharmathene. Tissue culture medium and reagents were from Biological Industries. Agarose-electrophoresis grade gel was from Invitrogen. Chloroform was from Bio-Rad Labratories. EDTA was from J.T. Baker.

Optical Characterization

Absorbance spectra were measured using a JASCO V-570 UV−Vis-NIR spectrophotometer. Photoluminescence experiments were performed using 500 nm for excitation wavelength with a Cary Eclipse fluorometer (Varian Inc.). The fluorescence QY of the nanocrystals was determined in toluene and aqueous solutions at room temperature by comparing their integrated emission to that of the organic fluorophore rhodamine 640 perchlorate dye in methanol solutions, with equal optical density at the excitation wavelength. The QY values were corrected for the differences in the refractive indices.

Ligand Exchange

MPA stock solution was prepared by mixing 40 μL of MPA (4.59×10^{-3} mol) with 1 mL of methanol and 50 mg of potassium hydroxide. A total of 100 μL of MPA stock solution was added to 1 mL of QDs in chloroform with an optical density of 1.5, and the solution was mixed. The chloroform solution flocculated and became turbid. An amount of 1.5 mL of basic TDW (pH 11−12) was added to the flocculent solution, which was mixed again. QDs were then extracted from the water phase.

Conjugation Procedure

Conjugation was attained by mixing 1 μg of rhBChE dimers (170 kDa) with QDs for 2 h in TDW (pH = 6, 200 μL final volume). The stoichiometry ratio for QD-rhBChE in the text refers to QDs per rhBChE dimer molecule.

Gel Electrophoresis

Samples were run on 0.5% agarose gel (Invitrogen) in 20 mM tris-acetate and 0.5 mM EDTA buffer (TAE). Bands were observed by exposure to UV light using a gel documentation system (UVIdoc GAS 9000 version 11; UVItec Limited).

DOI: 10.1021/cn1000827 | *ACS Chem. Neurosci.* (2011), *2*, 141–150

Structural Characterization

TEM measurements were carried out on QDs and QD-rhBChE conjugates using a Tecnai G^2 Spirit Twin T-12 transmission electron microscope with a tungsten filament running at an accelerating voltage of 120 keV. Conjugate preparations were deposited on carbon coated 400-mesh copper grids covered with a thin amorphous carbon film. QD-rhBChE samples were positively stained with 2.5% aqueous uranyl acetate.

Enzyme Activity Measurements

rhBChE hydrolytic activity involved adaptation of Ellman's colorimetric method(*54*) to a microtiter plate assay using *S*-butyrylthiocholine iodide as a substrate. Ellman's reagent, 0.5 mL of 30 mM DTNB, and 1.5 mL of 0.1 M phosphate buffer pH 7.4 were freshly prepared. Samples of 10 μL were placed in wells of a 96-well microplate followed by 180 μL of the Ellman's reagent and 10 μL of substrate (0.5 mmol/L final concentration). The reaction was monitored using a microplate spectrophotometer reader (SpectraFluor Plus; Tecan Group Ltd.) for at least 20 min at 405 nm wavelength at room temperature (22.5 °C). For the inhibitor sensitivity test, the samples were preincubated with 10 μL of 1 mM paraoxon for 20 min in the dark before substrate addition. Reaction rates were assessed from the linear portion of the reaction curves as changes of absorbance per minute. At each time interval, values were calculated separately for each sample in comparison with its own baseline. All samples were run in triplicate.

Cell Culture

bEnd.3 *Mus musculus* brain microvascular endothelial cells (ATCC number: CRL-2299, Manassas, VA) were cultured in a fully humidified atmosphere at 37 °C and 5% CO_2 in Dulbecco's modified Eagle medium (DMEM) containing 10% each fetal bovine serum (FBS), a mixture of 1% penicillin−streptomycin−amphotericin, and 2 mM L-glutamine. For confocal imaging, a medium without FBS was used.

Confocal Microscopy Live Cell Imaging

Cells were scanned using the FV-1000 confocal microscope (Olympus, Japan) equipped with an IX81 inverted microscope and an incubator (LIS, Switzerland) controlling temperature and CO_2 concentration. A 60×/1.35 oil immersion objective was used. QD fluorescence and nuclear staining with Hoechst 33342 was imaged using the 405 nm laser line for excitation and emission collection with 605−644 nm and 430−470 nm filters, respectively. Transmitted light DIC images were taken as well.

Supporting Information Available

Additional materials and methods which include the chemicals used, the synthesis of QDs, toxicity measurements, and UV light effect on rhBChE catalytic activity. This material is available free of charge via the Internet at http://pubs.acs.org.

Author Information

Corresponding Author

* (U.B.) Mailing address: The Institute of Chemistry and the Center for Nanoscience and Nanotechnology, The Hebrew University of Jerusalem, Edmond J. Safra Campus, Givat Ram, Jerusalem 91904. Telephone: 972-026584515. E-mail: banin@chem.ch.huji.ac.il. (H.S.) Mailing address: The Alexander Silberman Institute of Life Sciences and the Edmond and Lily Safra Center for Brain Sciences, The Hebrew University of Jerusalem, Edmond J. Safra Campus, Givat Ram, Jerusalem 91904. Telephone: 972-2-6585109. E-mail: soreq@cc.huji.ac.il.

Author Contributions

N.W. and I.S. designed, confirmed, and analyzed the experiments as well as wrote the first draft of the manuscript. I.L. contributed the quantum dot. U.B. and H.S. initiated, shaped, and supervised the research, and revised and extended the manuscript.

Funding Sources

This study was supported by the Israel Science Foundation Bio-Med Morasha Program (Grant # 1876/08) and The European Community (LSHG-CT-2006-037277) to H.S., and by the Converging Technologies Program administered by the Israel Science Foundation (Grant # 1704/07) to U.B. U.B. wishes to thank the Alfred and Erica Larisch Memorial Chair in Solar Energy.

Notes

We see no conflict of interest or bias in our affiliations, funding sources, and financial or management relationships that may constitute conflicts of interest.

Acknowledgment

The authors are grateful to Pharmathene, US for the recombinant human BChE, to Dr. Janet Macdonald for her assistance with the TEM imaging, and to Dr. Naomi Melamed-Book for assistance with the confocal imaging.

Abbreviations

Acetylcholine, ACh; butyrylcholinesterase, BChE; mercaptopropionic acid, MPA; nanoparticles, NPs; quantum dots, QDs; quantum yield, QY; recombinant human BChE, rhBChE; transmission electron microscopy, TEM; triple distilled water, TDW.

References

1. Mendel, B., and Rudney, H. (1943) Studies on Cholinesterase 1. Cholinesterase and pseudo-cholinesterase. *Biochem. J. 37*, 59–63.

2. Kalow, W., and Genest, K. (1957) A Method for the Detection of Atypical Forms of Human Serum Cholinesterase - Determination of Dibucaine Numbers. *Can. J. Biochem. Physiol. 35*, 339–346.

3. Lockridge, O., and Ladu, B. N. (1978) Comparison of Atypical and Usual Human-Serum Cholinesterase - Purification, Number of Active-Sites, Substrate Affinity, and Turnover Number. *J. Biol. Chem. 253*, 361–366.

4. Darvesh, S., Hopkins, D. A., and Geula, C. (2003) Neurobiology of butyrylcholinesterase. *Nat. Rev. Neurosci. 4*, 131–138.

5. Shute, C. C. D., and Lewis, P. R. (1963) Cholinesterase-Containing Systems of Brain of Rat. *Nature 199*, 1160–1164.

DOI: 10.1021/cn1000827 | *ACS Chem. Neurosci.* (2011), *2*, 141–150

6. Robinson, N. (1966) Friedreichs Ataxia - a Histochemical and Biochemical Study 0.2. Hydrolytic Enzymes. *Acta Neuropathol. 6*, 35–45.

7. Edwards, J. A., and Brimijoin, S. (1982) Divergent Regulation of Acetylcholinesterase and Butyrylcholinesterase in Tissues of the Rat. *J. Neurochem. 38*, 1393–1403.

8. Taylor, P. (1996) Agents acting at the neuromuscular junction and autonomic ganglia, in *Goodman and Gilman's The Pharmacological Basis of Therapeutics* (Hardman, J., Limbird, L., Molinoff, P., Ruddon, R., Eds.), pp 177−197, McGraw-Hill, New York.

9. Li, B., Stribley, J. A., Ticu, A., Xie, W. H., Schopfer, L. M., Hammond, P., Brimijoin, S., Hinrichs, S. H., and Lockridge, O. (2000) Abundant tissue butyrylcholinesterase and its possible function in the acetylcholinesterase knockout mouse. *J. Neurochem. 75*, 1320–1331.

10. Minic, J., Chatonnet, A., Krejci, E., and Molgo, J. (2003) Butyrylcholinesterase and acetylcholinesterase activity and quantal transmitter release at normal and acetylcholinesterase knockout mouse neuromuscular junctions. *Br. J. Pharmacol. 138*, 177–187.

11. Loewenstein-Lichtenstein Y, S. M., Glick D, Nørgaard-Pedersen B, Zakut H, Soreq H. (1995) Genetic predisposition to adverse consequences of anti-cholinesterases in 'atypical' BCHE carriers. *Nat. Med. 1*, 1082−1085.

12. Kalow, W., and Davies, R. O. (1959) The activity of various esterase inhibitors towards atypical human serum cholinesterase. *Biochem. Pharmacol. 1*, 183–192.

13. Prody, C. A., Dreyfus, P., Zamir, R., Zakut, H., and Soreq, H. (1989) De novo amplification within a "silent" human cholinesterase gene in a family subjected to prolonged exposure to organophosphorous insecticides. *Proc. Natl. Acad. Sci. U.S.A. 86*, 690–694.

14. Kutty, K. M., Redheendran, R., and Murphy, D. (1977) Serum-Cholinesterase - Function in Lipoprotein Metabolism. *Experientia 33*, 420–422.

15. Johnson, G., and Moore, S. W. (2000) Cholinesterases modulate cell adhesion in human neuroblastoma cells in vitro. *Int. J. Dev. Neurosci. 18*, 781–790.

16. Perry, E. K., Tomlinson, B. E., Blessed, G., Bergmann, K., Gibson, P. H., and Perry, R. H. (1978) Correlation of Cholinergic Abnormalities with Senile Plaques and Mental Test-Scores in Senile Dementia. *Br. Med. J. 2*, 1457–1459.

17. Mesulam, M. M., and Moran, M. A. (1987) Cholinesterases within Neurofibrillary Tangles Related to Age and Alzheimers-Disease. *Ann. Neurol. 22*, 223–228.

18. Podoly, E., Shalev, D. E., Shenhar-Tsarfaty, S., Bennett, E. R., Ben Assayag, E., Wilgus, H., Livnah, O., and Soreq, H. (2009) The Butyrylcholinesterase K Variant Confers Structurally Derived Risks for Alzheimer Pathology. *J. Biol. Chem. 284*, 17170–17179.

19. Ruberg, M., Rieger, F., Villageois, A., Bonnet, A. M., and Agid, Y. (1986) Acetylcholinesterase and Butyrylcholinesterase in Frontal-Cortex and Cerebrospinal-Fluid of Demented and Nondemented Patients with Parkinsons-Disease. *Brain Res. 362*, 83–91.

20. Benmoyal-Segal, L., Vander, T., Shifman, S., Bryk, B., Ebstein, R. P., Marcus, E.-L., Stessman, J., Darvasi, A., Herishanu, Y., Friedman, A., and Soreq, H. (2005) Acetylcholinesterase/ paraoxonase interactions increase the risk of insecticide-induced Parkinson's disease. *FASEB J. 19*, 452–454.

21. Richter, D., and Lee, M. (1942) Serum Choline Esterase and Anxiety. *J. Ment. Sci. 88*, 428–434.

22. Sklan, E. H., Lowenthal, A., Korner, M., Ritov, Y., Landers, D. M., Rankinen, T., Bouchard, C., Leon, A. S., Rice, T., Rao, D. C., Wilmore, J. H., Skinner, J. S., and Soreq, H. (2004) Acetylcholinesterase/paraoxonase genotype and expression predict anxiety scores in Health, Risk Factors, Exercise Training, and Genetics study. *Proc. Natl. Acad. Sci. U.S.A. 101*, 5512–5517.

23. Johnson, N. D., Duysen, E. G., and Lockridge, O. (2009) Intrathecal delivery of fluorescent labeled butyrylcholinesterase to the brains of butyrylcholinesterase knock-out mice: Visualization and quantification of enzyme distribution in the brain. *Neurotoxicology 30*, 386–392.

24. Chan, W. C. W., and Nie, S. M. (1998) Quantum dot bioconjugates for ultrasensitive nonisotopic detection. *Science 281*, 2016–2018.

25. Larson, D. R., Zipfel, W. R., Williams, R. M., Clark, S. W., Bruchez, M. P., Wise, F. W., and Webb, W. W. (2003) Water-soluble quantum dots for multiphoton fluorescence imaging in vivo. *Science 300*, 1434–1436.

26. Resch-Genger, U., Grabolle, M., Cavaliere-Jaricot, S., Nitschke, R., and Nann, T. (2008) Quantum dots versus organic dyes as fluorescent labels. *Nat. Methods 5*, 763–775.

27. Gruber, H. J., Hahn, C. D., Kada, G., Riener, C. K., Harms, G. S., Ahrer, W., Dax, T. G., and Knaus, H. G. (2000) Anomalous fluorescence enhancement of Cy3 and Cy3.5 versus anomalous fluorescence loss of Cy5 and Cy7 upon covalent linking to IgG and noncovalent binding to avidin. *Bioconjugate Chem. 11*, 696–704.

28. Griesbeck, O., Baird, G. S., Campbell, R. E., Zacharias, D. A., and Tsien, R. Y. (2001) Reducing the environmental sensitivity of yellow fluorescent protein - Mechanism and applications. *J. Biol. Chem. 276*, 29188–29194.

29. Shaner, N. C., Steinbach, P. A., and Tsien, R. Y. (2005) A guide to choosing fluorescent proteins. *Nat. Methods 2*, 905–909.

30. Medintz, I. L., Uyeda, H. T., Goldman, E. R., and Mattoussi, H. (2005) Quantum dot bioconjugates for imaging, labelling and sensing. *Nat. Mater. 4*, 435–446.

31. Michalet, X., Pinaud, F. F., Bentolila, L. A., Tsay, J. M., Doose, S., Li, J. J., Sundaresan, G., Wu, A. M., Gambhir, S. S., and Weiss, S. (2005) Quantum dots for live cells, in vivo imaging, and diagnostics. *Science 307*, 538–544.

32. Semonin, O. E., Johnson, J. C., Luther, J. M., Midgett, A. G., Nozik, A. J., and Beard, M. C. (2010) Absolute Photoluminescence Quantum Yields of IR-26 Dye, PbS, and PbSe Quantum Dots. *J. Phys. Chem. Lett. 1*, 2445–2450.

33. Leatherdale, C. A., Woo, W. K., Mikulec, F. V., and Bawendi, M. G. (2002) On the absorption cross section of CdSe nanocrystal quantum dots. *J. Phys. Chem. B 106*, 7619–7622.

34. Yu, W. W., Qu, L., Guo, W., and Peng, X. (2003) Experimental Determination of the Extinction Coefficient

DOI: 10.1021/cn1000827 | *ACS Chem. Neurosci.* (2011), *2*, 141–150

of CdTe, CdSe, and CdS Nanocrystals. *Chem. Mater. 15*, 2854–2860.

35. Peng, X. G., Schlamp, M. C., Kadavanich, A. V., and Alivisatos, A. P. (1997) Epitaxial growth of highly luminescent CdSe/CdS core/shell nanocrystals with photostability and electronic accessibility. *J. Am. Chem. Soc. 119*, 7019–7029.

36. Sun, Y. H., Liu, Y. S., Vernier, P. T., Liang, C. H., Chong, S. Y., Marcu, L., and Gundersen, M. A. (2006) Photostability and pH sensitivity of CdSe/ZnSe/ZnS quantum dots in living cells. *Nanotechnology 17*, 4469–4476.

37. Nida, D. L., Nitin, N., Yu, W. W., Colvin, V. L., Richards-Kortum, R. (2008) Photostability of quantum dots with amphiphilic polymer-based passivation strategies. *Nanotechnology 19*.

38. Nann, T. (2005) Phase-transfer of CdSe@ZnS quantum dots using amphiphilic hyperbranched polyethylenimine. *Chem. Commun*.1735–1736.

39. Yu, W. W., Chang, E., Falkner, J. C., Zhang, J. Y., Al-Somali, A. M., Sayes, C. M., Johns, J., Drezek, R., and Colvin, V. L. (2007) Forming biocompatible and nonaggregated nanocrystals in water using amphiphilic polymers. *J. Am. Chem. Soc. 129*, 2871–2879.

40. Gerion, D., Pinaud, F., Williams, S. C., Parak, W. J., Zanchet, D., Weiss, S., and Alivisatos, A. P. (2001) Synthesis and properties of biocompatible water-soluble silica-coated CdSe/ZnS semiconductor quantum dots. *J. Phys. Chem. B 105*, 8861–8871.

41. Derjaguin, B., and Landau, L. (1993) Theory of the Stability of Strongly Charged Lyophobic Sols and of the Adhesion of Strongly Charged-Particles in Solutions of Electrolytes. *Prog. Surf. Sci. 43*, 30–59.

42. Hoshino, A., Fujioka, K., Oku, T., Suga, M., Sasaki, Y. F., Ohta, T., Yasuhara, M., Suzuki, K., and Yamamoto, K. (2004) Physicochemical Properties and Cellular Toxicity of Nanocrystal Quantum Dots Depend on Their Surface Modification. *Nano Lett. 4*, 2163–2169.

43. Smith, A. M., Duan, H. W., Rhyner, M. N., Ruan, G., and Nie, S. M. (2006) A systematic examination of surface coatings on the optical and chemical properties of semiconductor quantum dots. *Phys. Chem. Chem. Phys. 8*, 3895–3903.

44. Gill, R., Willner, I., Shweky, I., and Banin, U. (2005) Fluorescence resonance energy transfer in CdSe/ZnS-DNA conjugates: Probing hybridization and DNA cleavage. *J. Phys. Chem. B 109*, 23715–23719.

45. Pinaud, F., King, D., Moore, H. P., and Weiss, S. (2004) Bioactivation and cell targeting of semiconductor CdSe/ZnS nanocrystals with phytochelatin-related peptides. *J. Am. Chem. Soc. 126*, 6115–6123.

46. Goldman, E. R., Balighian, E. D., Mattoussi, H., Kuno, M. K., Mauro, J. M., Tran, P. T., and Anderson, G. P. (2002) Avidin: A natural bridge for quantum dot-antibody conjugates. *J. Am. Chem. Soc. 124*, 6378–6382.

47. Mattoussi, H., Mauro, J. M., Goldman, E. R., Anderson, G. P., Sundar, V. C., Mikulec, F. V., and Bawendi, M. G. (2000) Self-assembly of CdSe-ZnS quantum dot bioconjugates using an engineered recombinant protein. *J. Am. Chem. Soc. 122*, 12142–12150.

48. Hermanson, G. T. (1996) *Bioconjugate Techniques*, Academic Press, New York.

49. Carbone, L., Nobile, C., De Giorgi, M., Sala, F. D., Morello, G., Pompa, P., Hytch, M., Snoeck, E., Fiore, A., Franchini, I. R., Nadasan, M., Silvestre, A. F., Chiodo, L., Kudera, S., Cingolani, R., Krahne, R., and Manna, L. (2007) Synthesis and micrometer-scale assembly of colloidal CdSe/CdS nanorods prepared by a seeded growth approach. *Nano Lett. 7*, 2942–2950.

50. Wuister, S. F., Swart, I., van Driel, F., Hickey, S. G., and Donega, C. D. (2003) Highly luminescent water-soluble CdTe quantum dots. *Nano Lett. 3*, 503–507.

51. Kolarich, D., Weber, A., Pabst, M., Stadlmann, J., Teschner, W., Ehrlich, H., Schwarz, H. P., and Altmann, F. (2008) Glycoproteomic characterization of butyrylcholinesterase from human plasma. *Proteomics 8*, 254–263.

52. Huang, Y.-J., Huang, Y., Baldassarre, H., Wang, B., Lazaris, A., Leduc, M., Bilodeau, A. S., Bellemare, A., Cote, M., Herskovits, P., Touati, M., Turcotte, C., Valeanu, L., Lemee, N., Wilgus, H., Begin, I., Bhatia, B., Rao, K., Neveu, N., Brochu, E., Pierson, J., Hockley, D. K., Cerasoli, D. M., Lenz, D. E., Karatzas, C. N., and Langermann, S. (2007) Recombinant human butyrylcholinesterase from milk of transgenic animals to protect against organophosphate poisoning. *Proc. Natl. Acad. Sci. U.S.A. 104*, 13603–13608.

53. Ngamelue, M. N., Homma, K., Lockridge, O., and Asojo, O. A. (2007) Crystallization and X-ray structure of full-length recombinant human butyrylcholinesterase. *Acta Crystallogr., Sect. F: Struct. Biol. Cryst. Commun. 63*, 723–727.

54. Ellman, G. L., Courtney, K. D., Andres, V., and Featherstone, R. M. (1961) A New and Rapid Colorimetric Determination of Acetylcholinesterase Activity. *Biochem. Pharmacol. 7*, 88–95.

55. Pompella, A., Visvikis, A., Paolicchi, A., De Tata, V., and Casini, A. F. (2003) The changing faces of glutathione, a cellular protagonist. *Biochem. Pharmacol. 66*, 1499–1503.

56. Baumle, M., Stamou, D., Segura, J. M., Hovius, R., and Vogel, H. (2004) Highly fluorescent streptavidin-coated CdSe nanoparticles: Preparation in water, characterization, and micropatterning. *Langmuir 20*, 3828–3831.

57. Qian, H. F., Dong, C. Q., Weng, J. F., and Ren, J. C. (2006) Facile one-pot synthesis of luminescent, water-soluble, and biocompatible glutathione-coated CdTe nanocrystals. *Small 2*, 747–751.

58. Harel, M., Schalk, I., Ehret-Sabatier, L., Bouet, F., Goeldner, M., Hirth, C., Axelsen, P. H., Silman, I., and Sussman, J. L. (1993) Quaternary ligand binding to aromatic residues in the active-site gorge of acetylcholinesterase. *Proc. Natl. Acad. Sci. U.S.A. 90*, 9031–9035.

59. Perrier, A. L., Massoulie, J., and Krejci, E. (2002) PRiMA: The membrane anchor of acetylcholinesterase in the brain. *Neuron 33*, 275–285.

60. Bon, S., Ayon, A., Leroy, J., and Massoulie, J. (2003) Trimerization domain of the collagen tail of acetylcholinesterase. *Neurochem. Res. 28*, 523–535.

61. Li, H., Schopfer, L. M., Masson, P., and Lockridge, O. (2008) Lamellipodin proline rich peptides associated with

DOI: 10.1021/cn1000827 | *ACS Chem. Neurosci.* (2011), *2*, 141–150

native plasma butyrylcholinesterase tetramers. *Biochem. J. 411*, 425–432.

62. Darvesh, S., and Hopkins, D. A. (2003) Differential distribution of butyrylcholinesterase and acetylcholinesterase in the human thalamus. *J. Comp. Neurol. 463*, 25–43.

63. Geula, C., and Nagykery, N. (2007) Butyrylcholinesterase activity in the rat forebrain and upper brainstem: Postnatal development and adult distribution. *Exp. Neurol. 204*, 640–657.

64. Ben Assayag, E., Shenhar-Tsarfaty, S., Ofek, K., Soreq, L., Bova, I., Shopin, L., Berg, R. M. G., Berliner, S., Shapira, I., Bornstein, N. M., and Soreq, H. (2010) Serum Cholinesterase Activities Distinguish between Stroke Patients and Controls and Predict 12-Month Mortality. *Mol. Med. 16*, 278–286.

65. Su, Y., He, Y., Lu, H., Sai, L., Li, Q., Li, W., Wang, L., Shen, P., Huang, Q., and Fan, C. (2009) The cytotoxicity of cadmium based, aqueous phase - Synthesized, quantum dots and its modulation by surface coating. *Biomaterials 30*, 19–25.

DOI: 10.1021/cn1000827 | *ACS Chem. Neurosci.* (2011), *2*, 141–150